

Ongoing Radio Space-Weather Science Studies Using the LOw Frequency ARray (LOFAR) and Three-Dimensional (3-D) Modelling Techniques

Mario M. Bisi (Mario.Bisi@stfc.ac.uk) (1), Richard A. Fallows (2),
Charlotte Sobey (2), Tarraneh Eftekhari (2,3), Elizabeth A. Jensen (4),
Bernard V. Jackson (5), Hsiu-Shan Yu (5), and Dusan Odstrcil (6,7).

(1) RAL Space, Science and Technology Facilities Council, Rutherford Appleton Laboratory, Harwell Oxford,
Didcot, Oxfordshire, OX11 0QX, England, UK

(2) ASTRON, the Netherlands Institute for Radio Astronomy, Postbus 2, 7990 AA Dwingeloo, The Netherlands

(3) University of New Mexico, Albuquerque, NM 87131, USA

(4) Planetary Science Institute, 1700 East Fort Lowell, Suite 106, Tucson, AZ 85719-2395, USA

(5) Center for Astrophysics and Space Science, University of California, San Diego, La Jolla, CA, 92093-0424, USA

(6) NASA Goddard Space Flight Center, Greenbelt, MD, USA

(7) School of Physics, Astronomy, and Computational Sciences, George Mason University, 4400 University Drive,
Fairfax, VA 22030-4444, USA.

Outline

- ❖ Brief Introduction to the Multi-Site Interplanetary Scintillation (IPS) Experiment (Radio Heliospheric Imaging)
 - ❖ UCSD 3-D Computer Assisted Tomography
 - ❖ IPS Developments with LOFAR
- ❖ Heliospheric Faraday Rotation (FR) Determination and Verification
 - Developments with LOFAR
 - ❖ Radio Heliospheric Modelling Developments: MHD and 3-D Tomography
 - ❖ HELCATS WP7 – T7.1
 - ❖ Brief Summary

Brief Introduction to the Multi-Site Interplanetary Scintillation (IPS) Experiment (Radio Heliospheric Imaging)

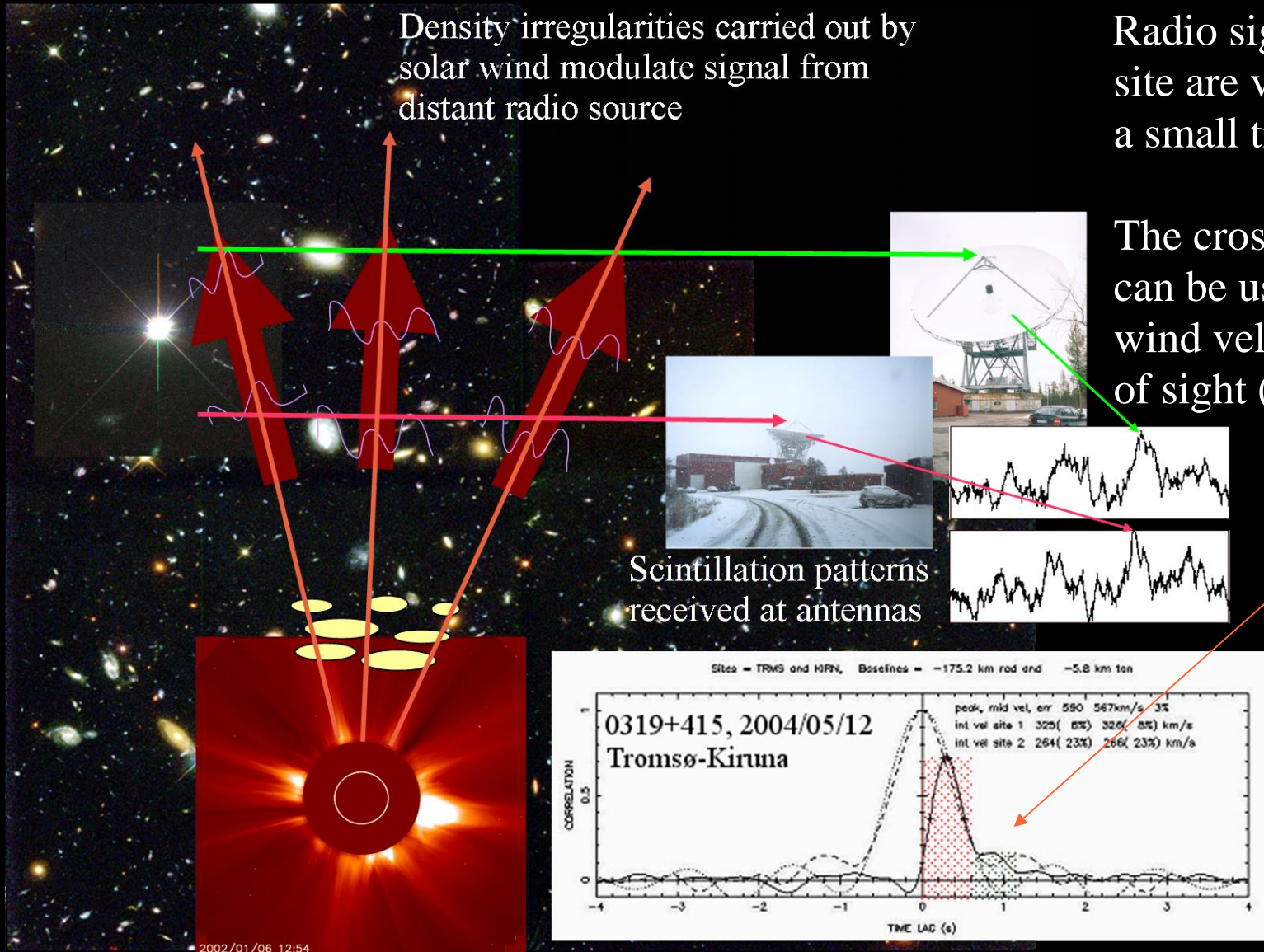
- *e.g.* see M.M. Bisi, “Planetary, heliospheric, and solar science with radio scintillation”, Chapter 13 of Heliophysics Volume IV “Stars, Astrospheres, and Planetary Environments”, Editors C.J. Schrijver, F. Bagenal, and J.J. Sojka, Cambridge University Press, in-press, 2015.

Multi-Site IPS

Density irregularities carried out by solar wind modulate signal from distant radio source

Radio signals received at each site are very similar except for a small time-lag.

The cross-correlation function can be used to infer the solar wind velocity(s) across the line of sight (LOS).



Hubble Deep Field – HST (WFPC2) 15/01/96 – Courtesy of R. Williams and the HDF Team and NASA

IPS is most-sensitive at and around the P-Point of the LOS to the Sun and is only sensitive to the component of flow that is perpendicular to the LOS; it is variation in intensity of astronomical radio sources on timescales of ~ 0.1 s to ~ 10 s that is observed.

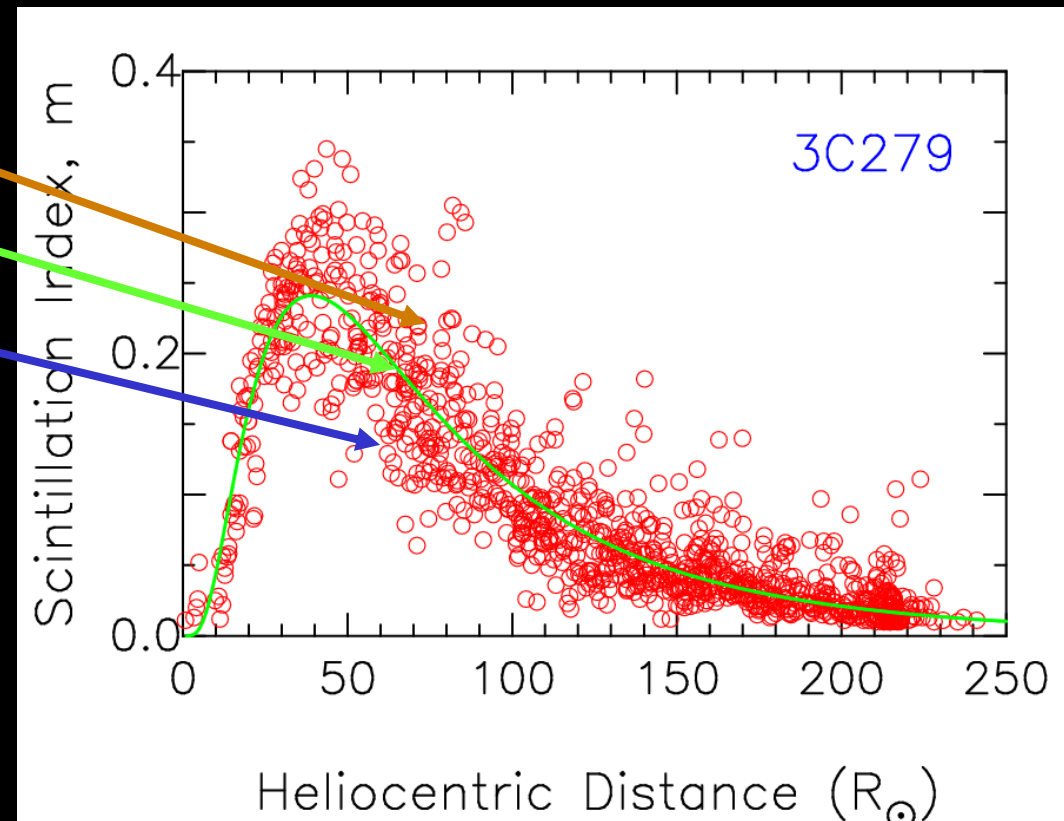
IPS (g -level/density)

Density Turbulence

- ❖ Scintillation index, m , is a measure of level of turbulence
- ❖ Normalized Scintillation index, $g = m(R) / \langle m(R) \rangle$

- $g > 1 \rightarrow$ enhancement in δN_e
- $g \approx 1 \rightarrow$ ambient level of δN_e
- $g < 1 \rightarrow$ rarefaction in δN_e

(Courtesy of Periasamy K. Manoharan)



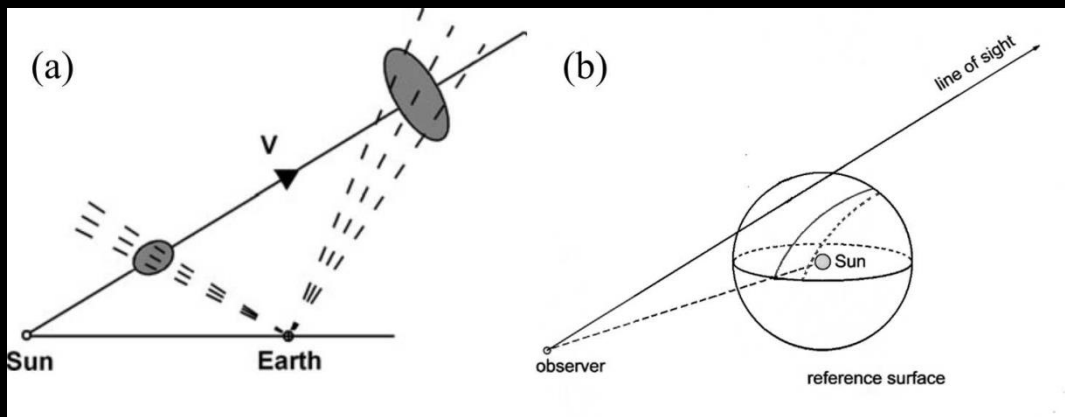
Scintillation enhancement with respect to the ambient wind identifies the presence of a region of increased turbulence/density and possible CME along the line-of-sight to the radio source

UCSD 3-D Computer Assisted Tomography

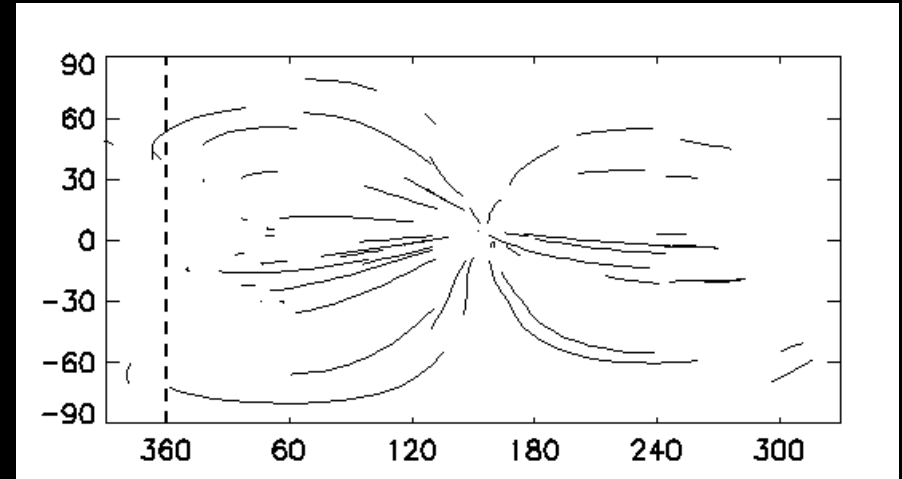
- *e.g.* see M.M. Bisi, “Planetary, heliospheric, and solar science with radio scintillation”, Chapter 13 of Heliophysics Volume IV “Stars, Astrospheres, and Planetary Environments”, Editors C.J. Schrijver, F. Bagenal, and J.J. Sojka, Cambridge University Press, in-press, 2015.

UCSD 3-D Tomography Simple View

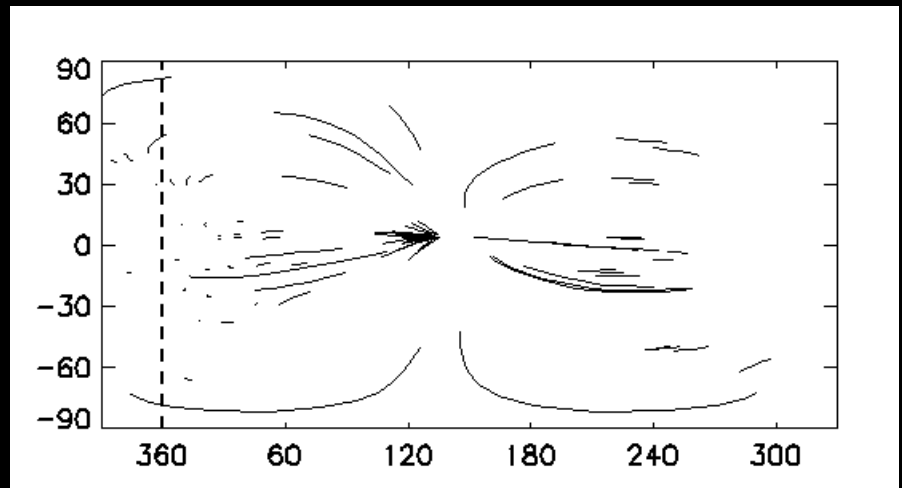
Heliospheric C.A.T. Analyses:
example line-of-sight distribution
for each sky location to form the
source surface of the 3D
reconstruction.



STELab IPS



13 July 2000



14 July 2000

IPS Developments with LOFAR

The LOW Frequency ARray (LOFAR)



LOFAR superterp, NL (top) and
LOFAR Chilbolton, UK (bottom).



LOFAR High-Band observes 110 MHz to ~250 MHz and LOFAR Low-Band observes ~10 MHz to ~90 MHz. Map (below) of operational (green) and upcoming (yellow) LOFAR stations across Europe. Pathfinder to the Square Kilometre Array (SKA).

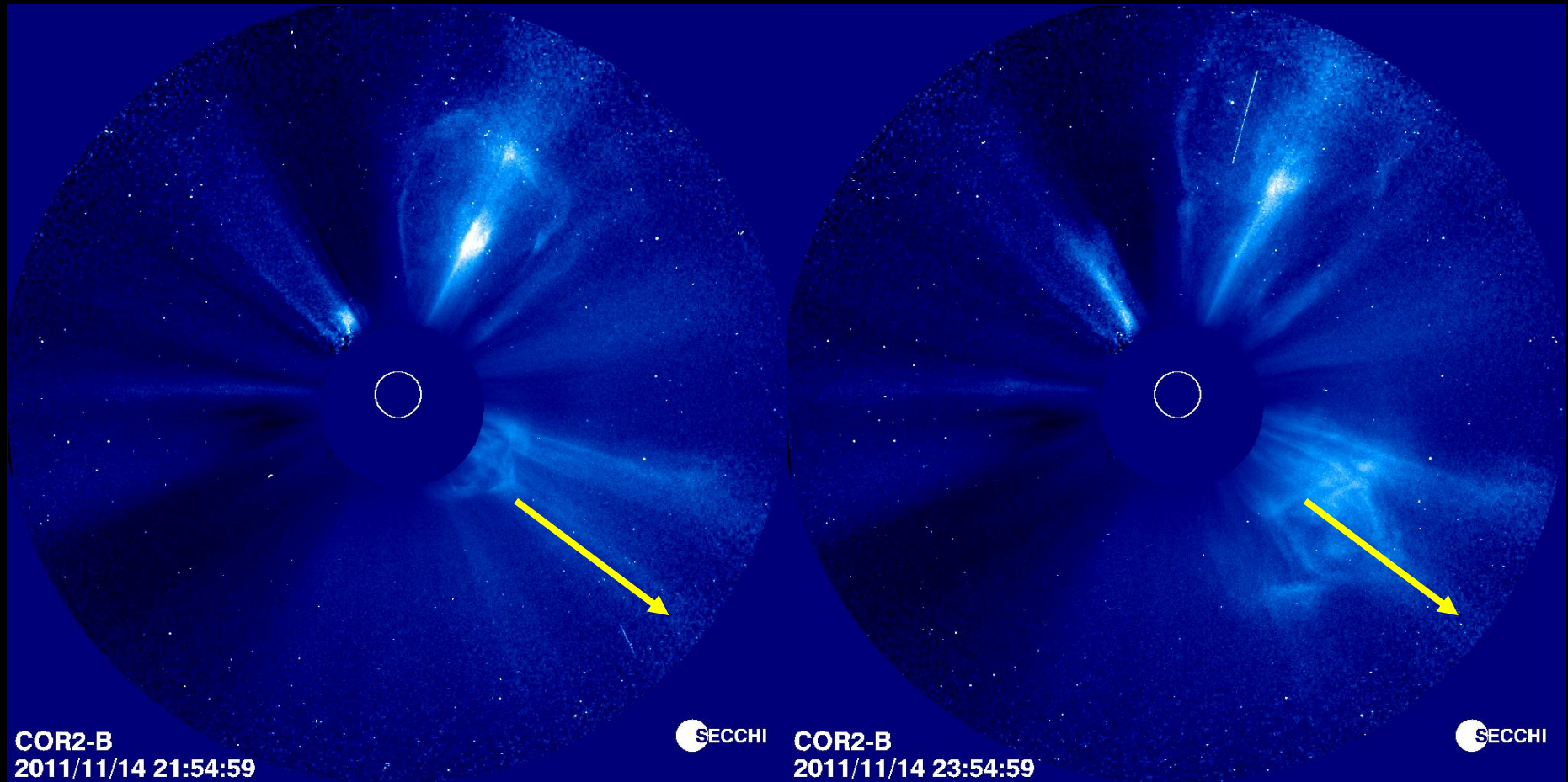


IPS with LOFAR: The First CME Detection

- R.A. Fallows, A. Asgekar, M.M. Bisi, A.R. Breen, S. ter-Veen, and on behalf of the LOFAR Collaboration, “The Dynamic Spectrum of Interplanetary Scintillation: First Solar Wind Observations on LOFAR”, Solar Physics “Observations and Modelling of the Inner Heliosphere” Topical Issue (Guest Editors M.M. Bisi, R.A. Harrison, and N. Lugaz), 285 (1-2), 127-139, 2013.

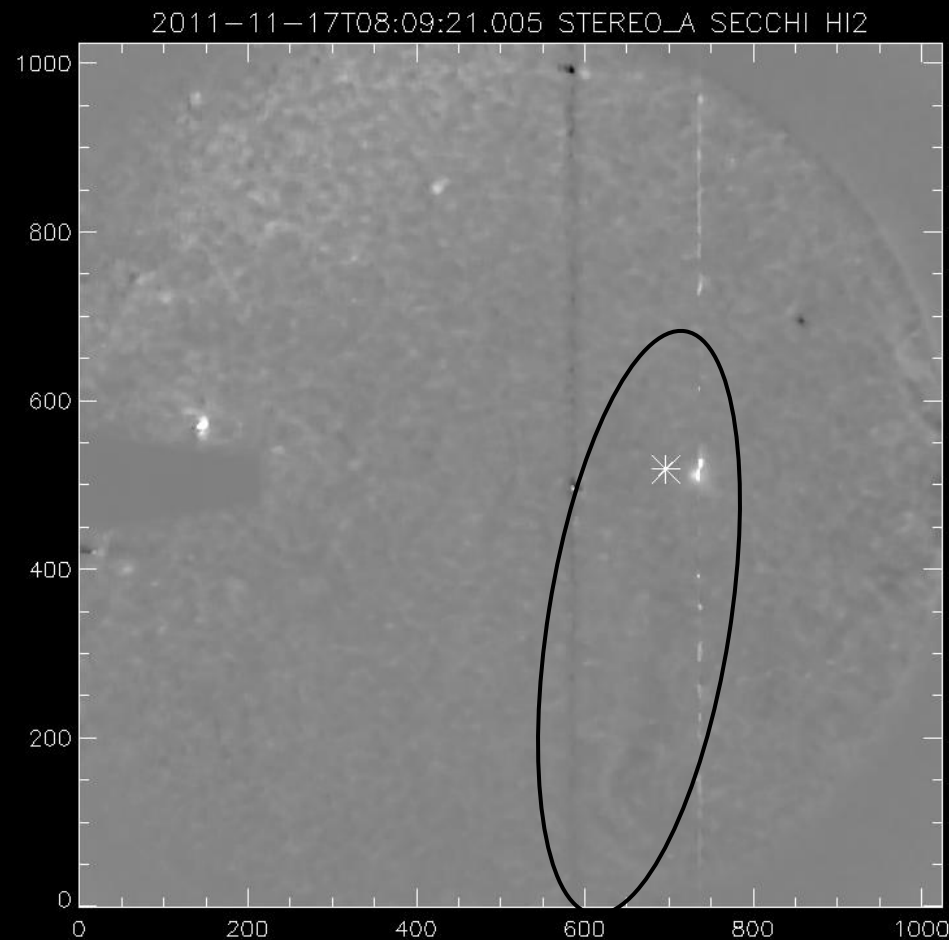
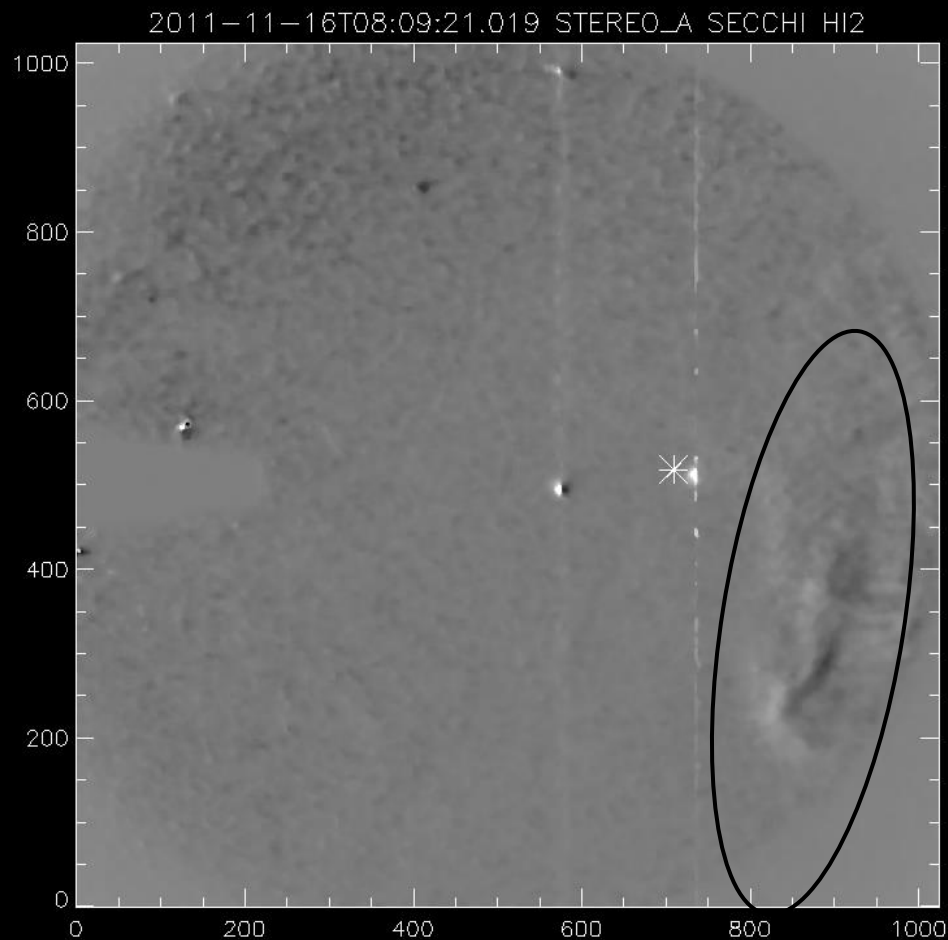
Taken from – M.M. Bisi, S.A. Hardwick, R.A. Fallows, J.A. Davies, R.A. Harrison, E.A. Jensen, H. Morgan, C.-C. Wu, A. Asgekar, M. Xiong, E. Carley, G. Mann, P.T. Gallagher, A. Kerdraon, A.A. Konovalenko, A. MacKinnon, J. Magdalenic, H.O. Rucker, B. Thide, C. Vocks, *et al.*, “The First Coronal Mass Ejection Observed with the LOw Frequency ARray (LOFAR)”, submitted to The Astrophysical Journal Supplementary Series, (and references therein), 2014/2015.

STEREO COR2-B CME Observations



- ❖ STEREO COR2 imagery of the CME seen to be going to the South-West from this viewpoint, *i.e.* South and Mars/Earth-ward (to the right of each image). Left: COR2-B on 14/11/11 at 21:54:59UT and Right: COR2-B on 14/11/11 at 23:54:59UT.

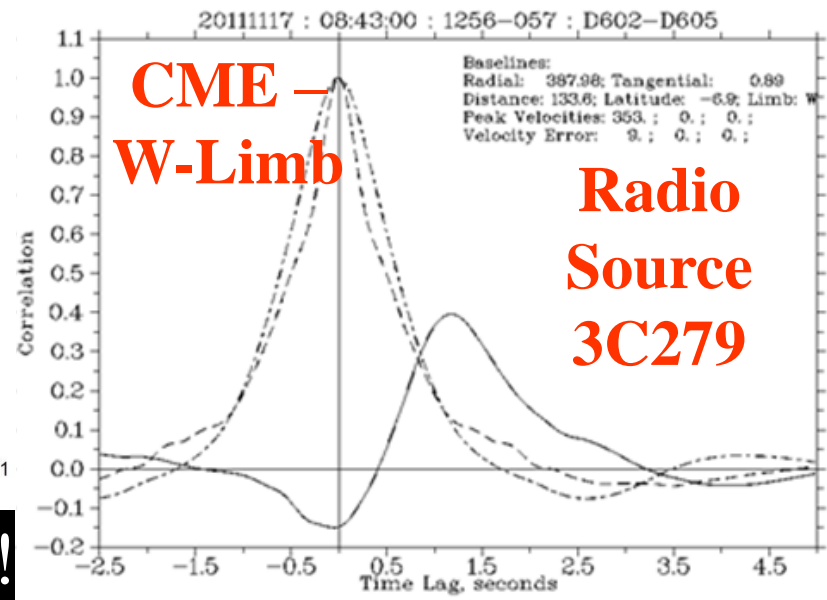
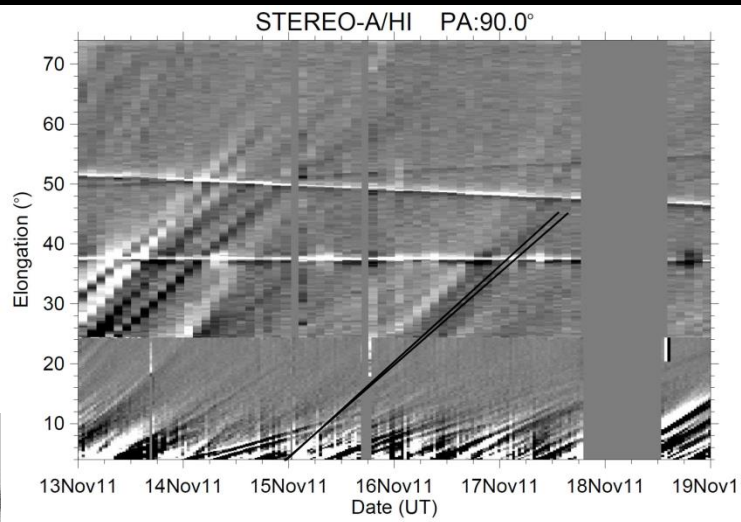
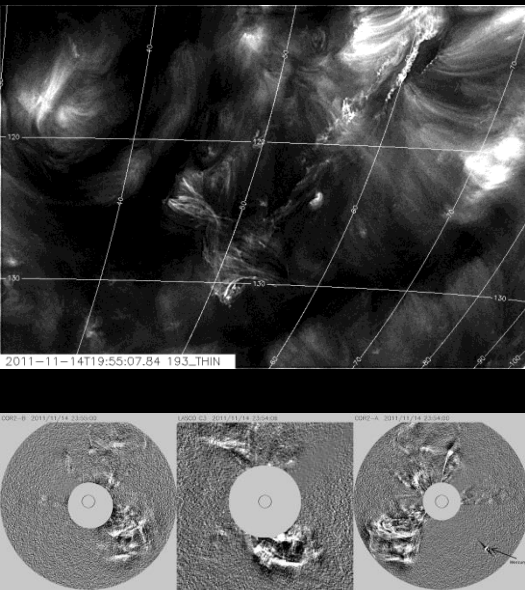
STEREO-A HI Observations of the CME



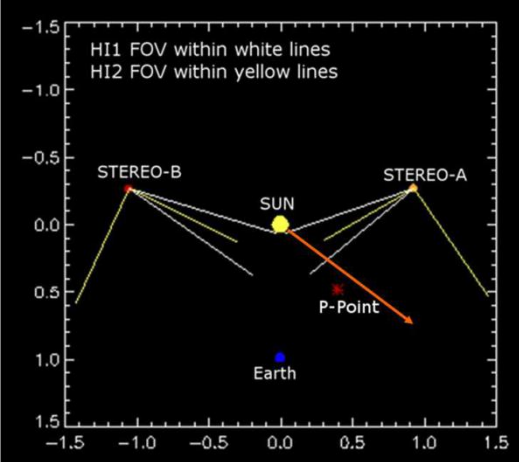
- ❖ STEREO-A HI imagery shows the Northern-most flank of the CME (inside the ellipse) crossing over the line of sight (*) to the radio source at the same time as the LOFAR observation of IPS.

The First CME with LOFAR...

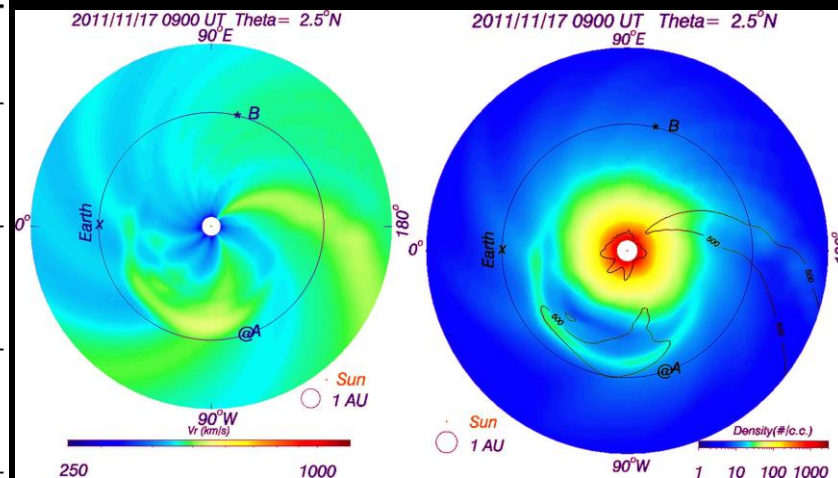
- Observations of J1256-057 (3C279) detecting a CME with LOFAR on 17 November 2011 and (briefly) its comparison so far with other remote-sensing observations and modelling.



Fully-consistent Results!



Model Used:	Best Fit in Radial Velocity (km s ⁻¹):	Error in Radial Velocity (km s ⁻¹):
<i>Front:</i>		
Fixed Phi	342.22	12.00
SSEF (30°)	348.83	12.00
Harmonic Mean	352.35	11.00
<i>Middle:</i>		
Fixed Phi	338.36	10.00
SSEF (30°)	343.61	10.00
Harmonic Mean	346.11	9.00
<i>Rear:</i>		
Fixed Phi	335.83	9.00
SSEF (30°)	343.53	8.00
Harmonic Mean	348.37	8.00



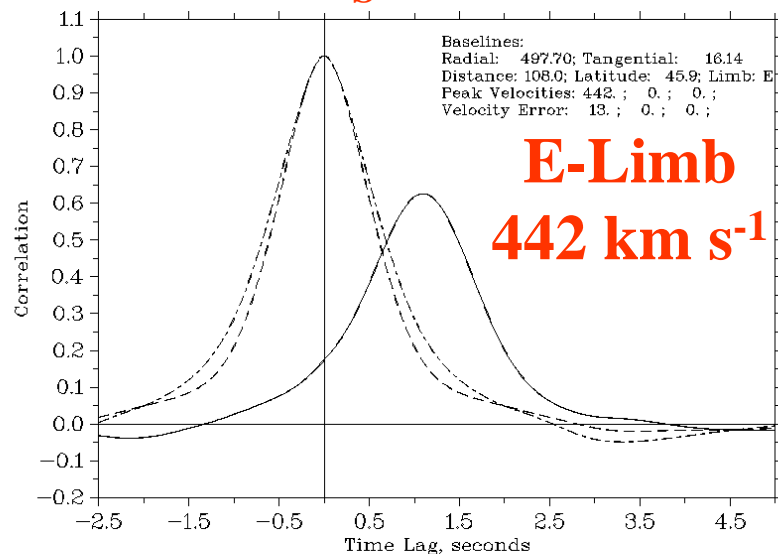
Our Second Coronal Mass Ejection (CME) with LOFAR...

- Investigations are ongoing.

LOFAR Observations of IPS on 03 June 2013

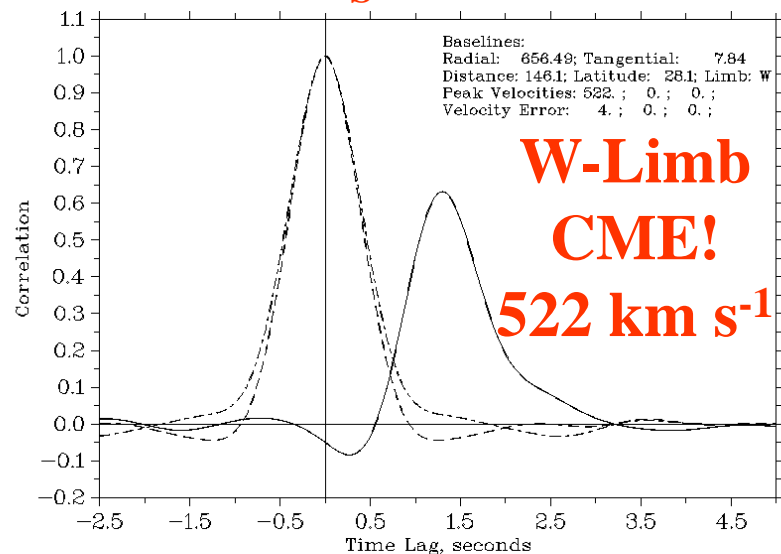
20130603 : 07:50:00 : 3C147 : F606-U608

108.0 R_S at 45.9° Lat.



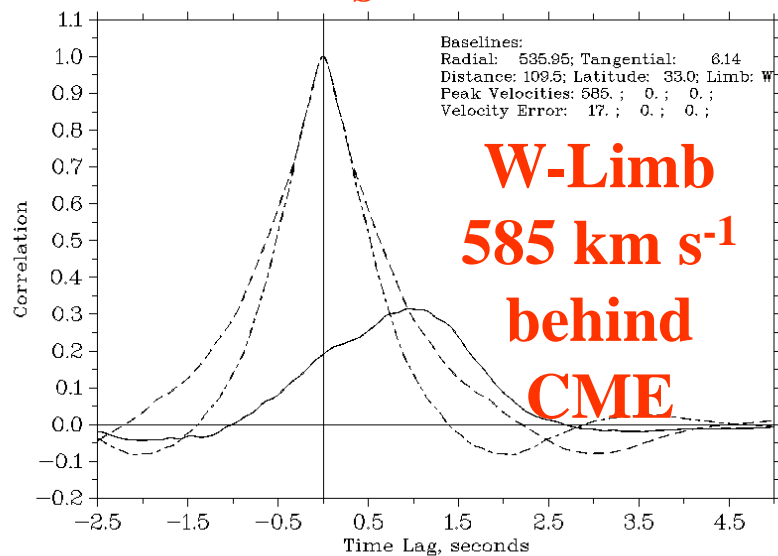
20130603 : 06:45:00 : 3C48 : D602-F606

146.1 R_S at 28.1° Lat.



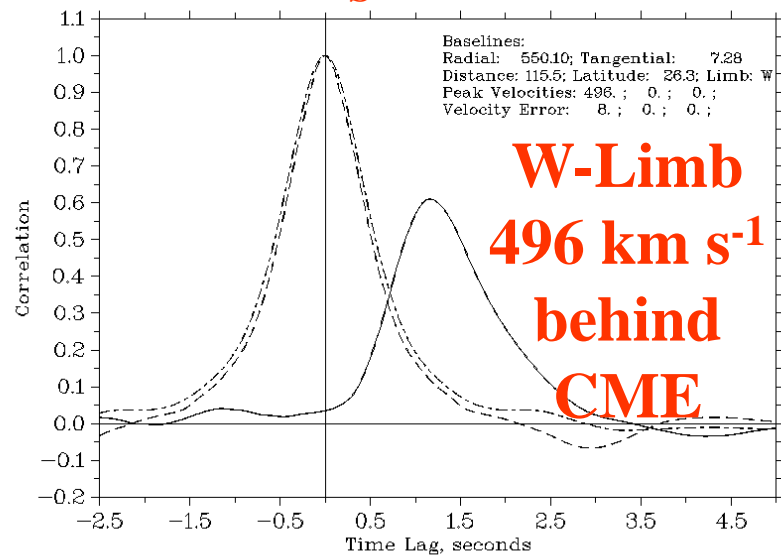
20130603 : 08:40:00 : 3C68.2 : D605-U608

109.5 R_S at 33.0° Lat.



20130603 : 09:26:00 : 3C67 : D605-U608

115.5 R_S at 26.3° Lat.



**Heliospheric Faraday Rotation (FR)
Determination and Verification
Developments with LOFAR**

LOFAR Heliospheric Faraday Rotation Observations

LOFAR heliospheric Faraday rotation (FR) observations to date are as follows...

Crab Nebula/3C144 (15 minutes of FR each time, plus 60 minutes of IPS on 02 July 2014 only):

- ❖ 02 July 2014 (10:40UT) – P-Point of $69 R_S$, 16.2° , Heliocentric Lat. -4.4° .
- ❖ 11 July 2014 (10:00UT) – P-Point of $104 R_S$, 24.8° , Heliocentric Lat. -2.8° .
- ❖ 22 July 2014 (12:00UT) – P-Point of $146 R_S$, 35.3° , Heliocentric Lat. -1.8° .

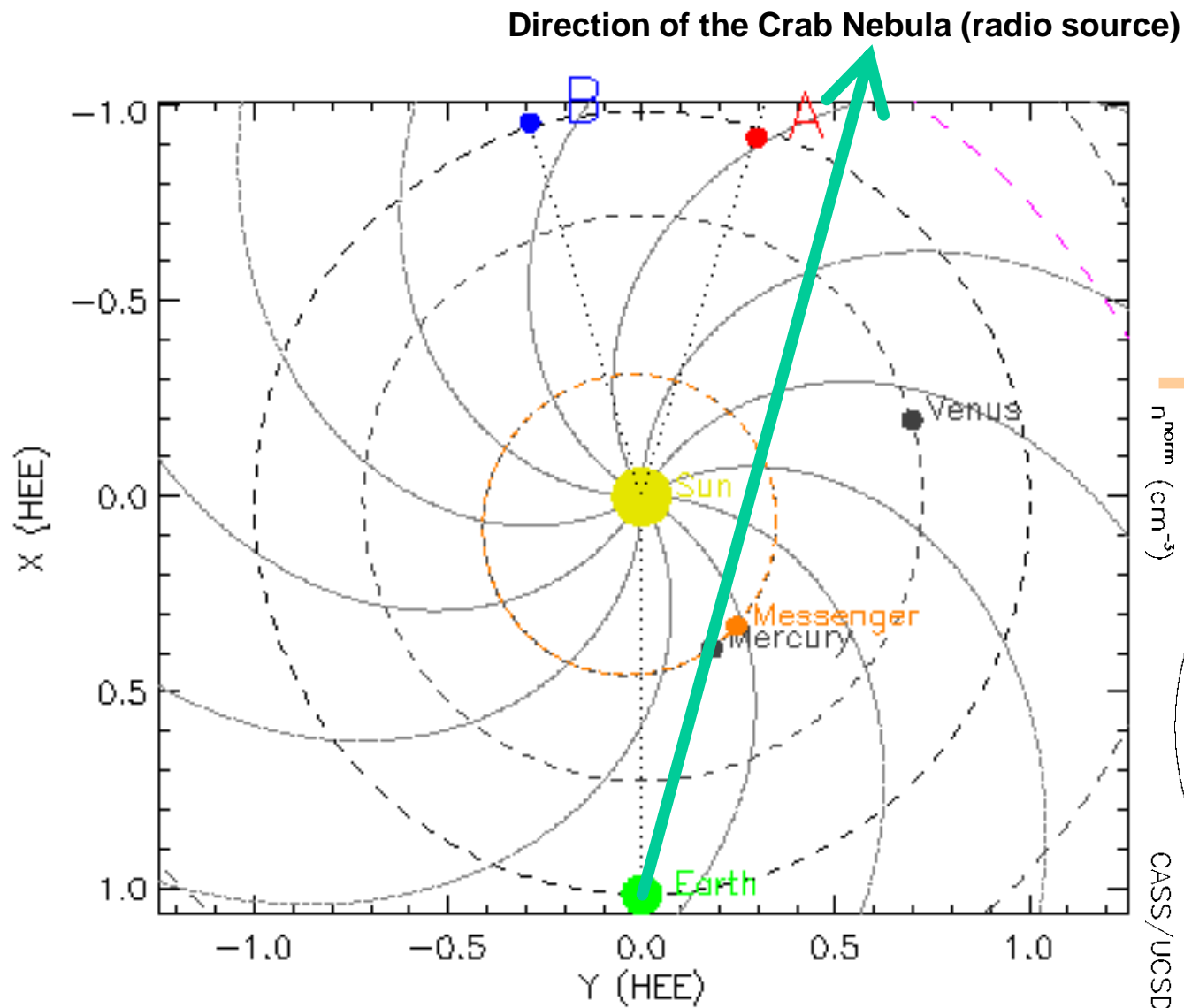
PSR J1022+1001:

- ❖ 13 August 2014 (13:00UT) – P-Point of $43.6 R_S$, 11.6° , and an extended observation of 140 minutes split into 20-minute intervals yet to be fully investigated in terms of the context of the observation.

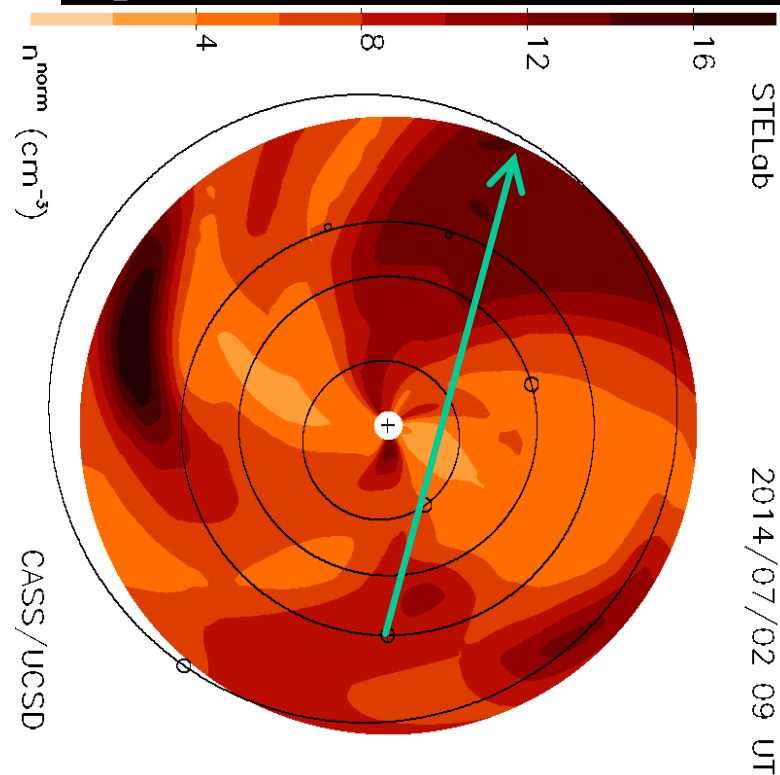
**Combined IPS (60 minutes) and
FR (15 minutes) Observations
of the Crab Nebula
(3C144/PSR B0531+21/PSR J0534+2200)
a few Degrees North of the Ecliptic on the
Sky Using LOFAR International Stations
Plus the Core, Respectively, on 02 July 2014
Commencing at 10:40UT**

- Work in progress – publications soon to be in preparation.

Inner-Heliosphere Ecliptic Context (1)



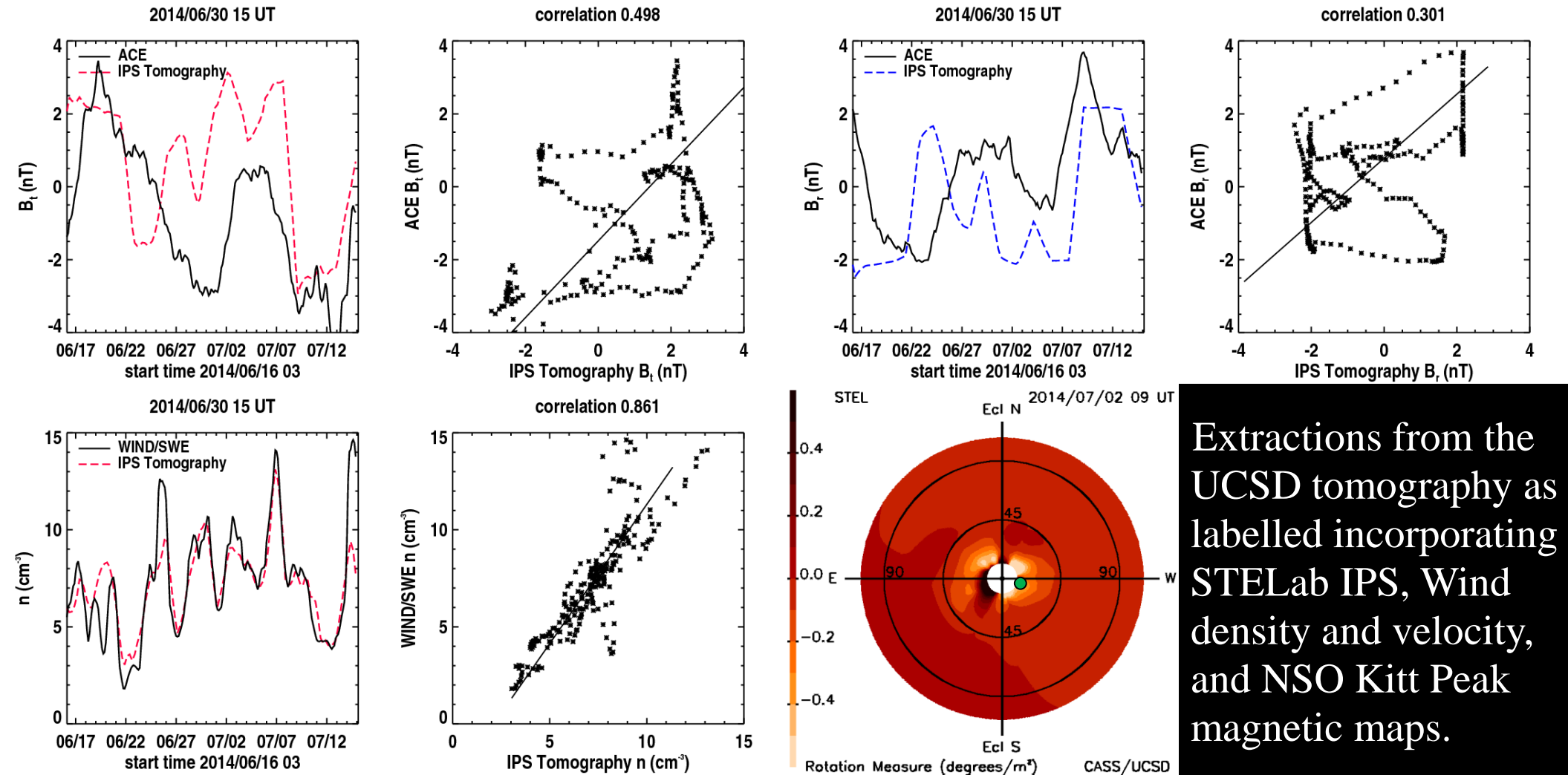
Density at Mercury from the UCSD tomography (using STELab IPS and Wind data) with the $1/R^2$ put back in (since the below image is normalised to 1 AU) provides $n = 31.9 \text{ cm}^{-3}$ (low).



2014/07/02 09 UT

- ❖ Left-hand Image courtesy of the STEREO Science Center —
- Where is STEREO? (http://stereo-ssc.nascom.nasa.gov/cgi-bin/make_where_gif)

Inner-Heliosphere Ecliptic Context (2)

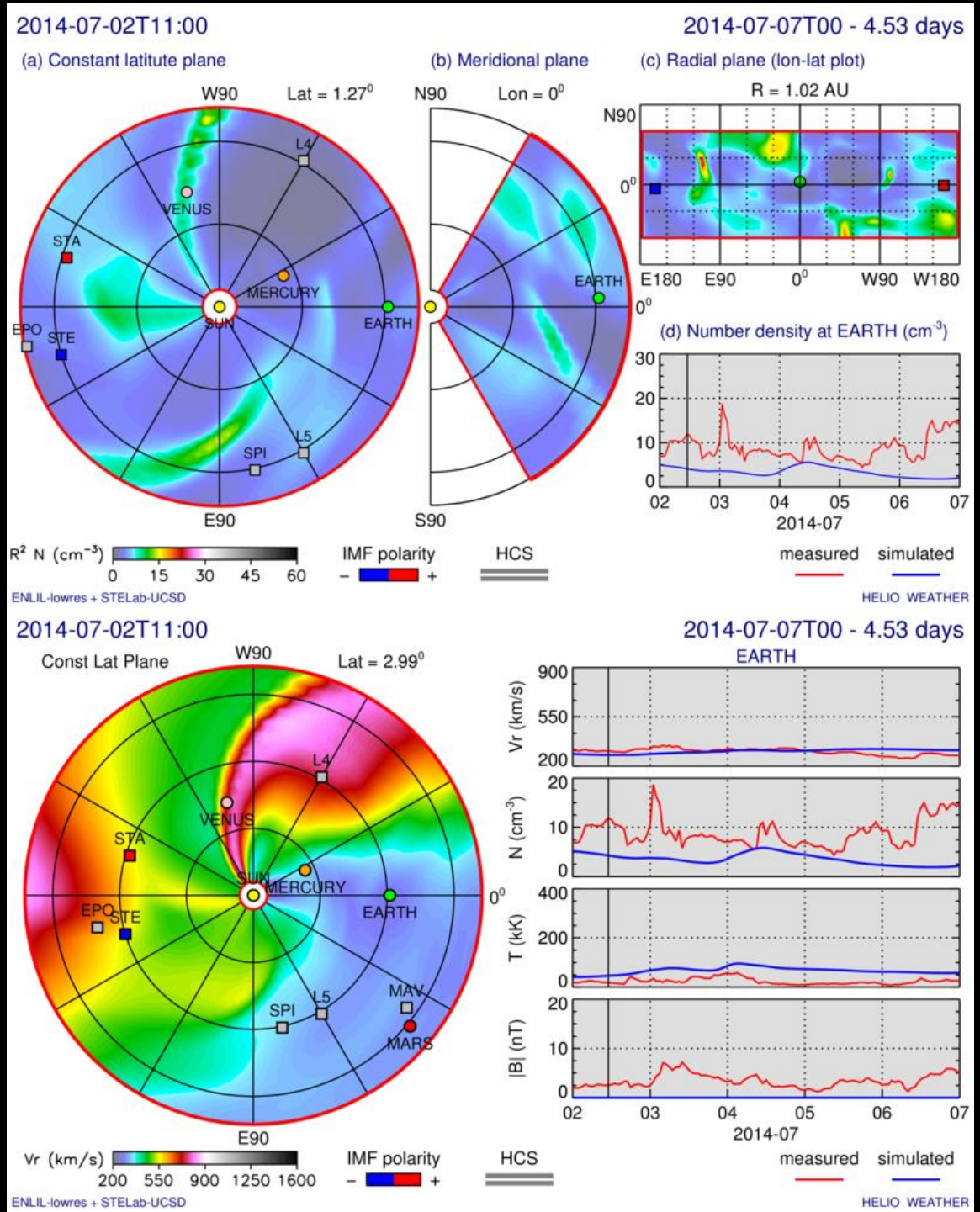


Extractions from the UCSD tomography as labelled incorporating STELab IPS, Wind density and velocity, and NSO Kitt Peak magnetic maps.

- ❖ MESSENGER data (courtesy of Dan Gershman, and Jim Raines) for context verification show a velocity $\sim 400 \text{ km s}^{-1}$, but density information is, unfortunately, not available for this period here.

Inner-Heliosphere Ecliptic Context (3)

- ❖ ENLIL MHD modelling using the UCSD IPS tomography as input to drive the model (IPS-driven ENLIL) as opposed to using the traditional WSA as input.
- ❖ Very-preliminary results suggest this provides an improved background solar-wind environment in the MHD modelling.



LOFAR Observing Characteristics

- ❖ Central observing frequency: 149.609375 MHz ($\lambda \sim 2$ m).
- ❖ Observing bandwidth: 78.125 MHz.
- ❖ IPS analyses over 15-minute integration times (10:40UT-10:55UT) – only the first 15 minutes used here to match the time of the pulsar observation.
- ❖ Pulsar observation analysed by folding the whole data set to obtain the polarised pulse profiles and then these are modelled using an RM fitting routine.
- ❖ RM is thus calculated on the integrated 15-minute observation.
- ❖ Implications for Space-Weather forecasting at the Earth.
- ❖ LOFAR observations of IPS using the international stations yielded a velocity of around 285 km s^{-1} .

Preliminary RM and FR (back-of-envelope calculations)

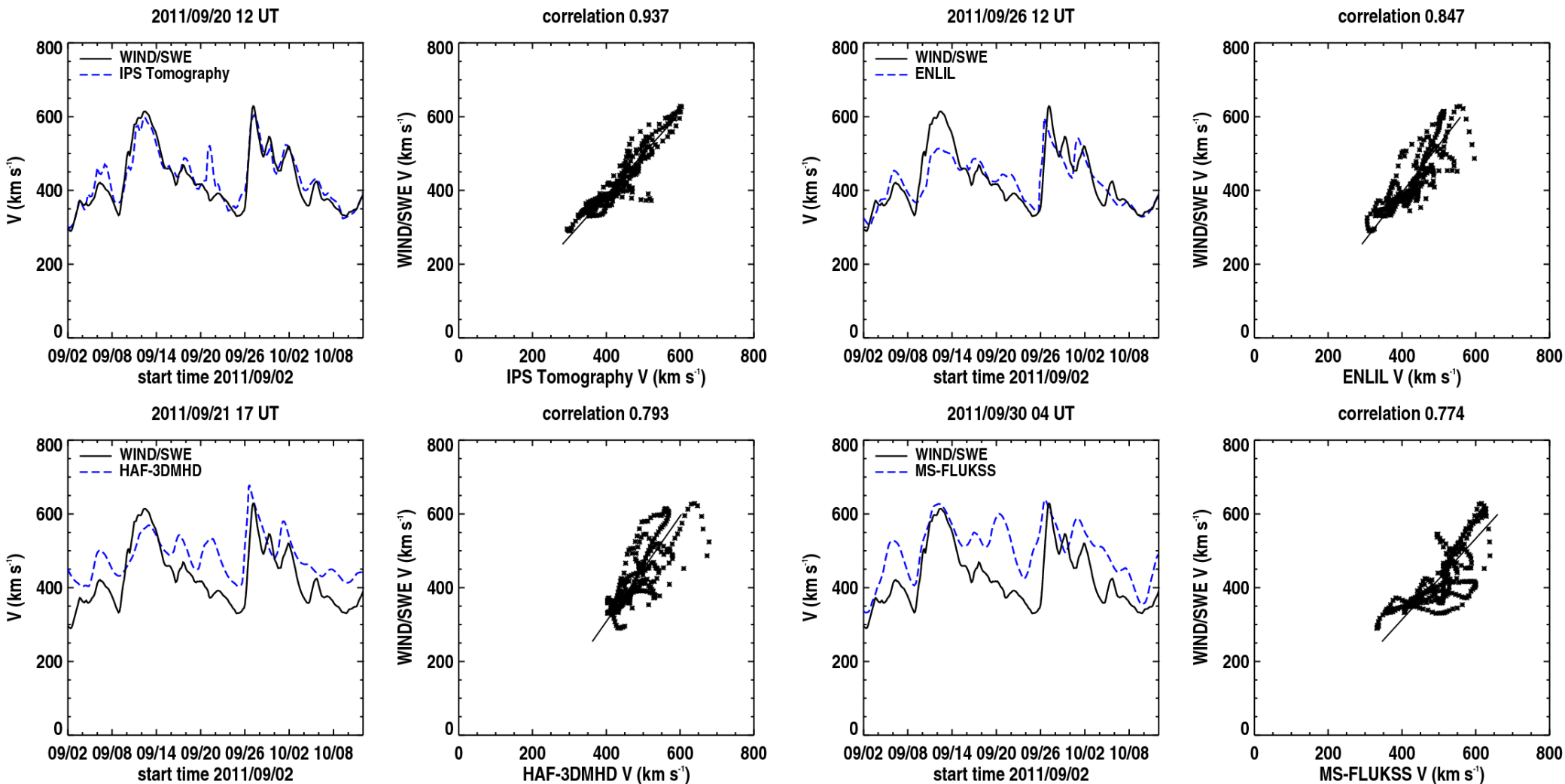
- ❖ The observed RM was: $-42.0571 \pm 0.02 \text{ rad m}^{-2}$.
- ❖ The expected RM of the Crab (at this frequency range) is expected to be: $-45.50848 \text{ rad m}^{-2}$ (based on anti-solar observations taken during February 2014).
- ❖ The modelled ionospheric RM was: $3.11127 \pm 0.12935 \text{ rad m}^{-2}$.
- ❖ The remaining RM, assumed due to be from the slow solar wind, is: $-0.34011 \pm 0.15589 \text{ rad m}^{-2}$, *i.e.* $-0.34 \pm 0.16 \text{ rad m}^{-2}$ (high?).
- ❖ Thus, using $\text{FR} = \lambda^2 \text{RM}$ (and just using the central frequency), the resulting FR is roughly: -1.36 rad .
- ❖ UCSD model RM result is \sim $-0.3^\circ \text{ m}^{-2}$ (factor $\sim 1/57$ of LOFAR)?
- ❖ Simplification: $\text{RM} = 0.002 \times n_e[\text{cm}^{-3}] \times B[\text{nT}] \times L[\text{AU}]^\circ \text{ m}^{-2}$
where L is the contributing integration length along line of sight
 $= 0.002 \times 80 \times -150 \times 0.4 =$ $-9.6^\circ \text{ m}^{-2}$ ($-0.168 \text{ rad m}^{-2}$) (high?).

Radio Heliospheric Modelling Developments: MHD and 3-D Tomography

Inclusion of *in-situ* data into the UCSD Tomography and using the Tomography Source Surface to Drive MHD Models

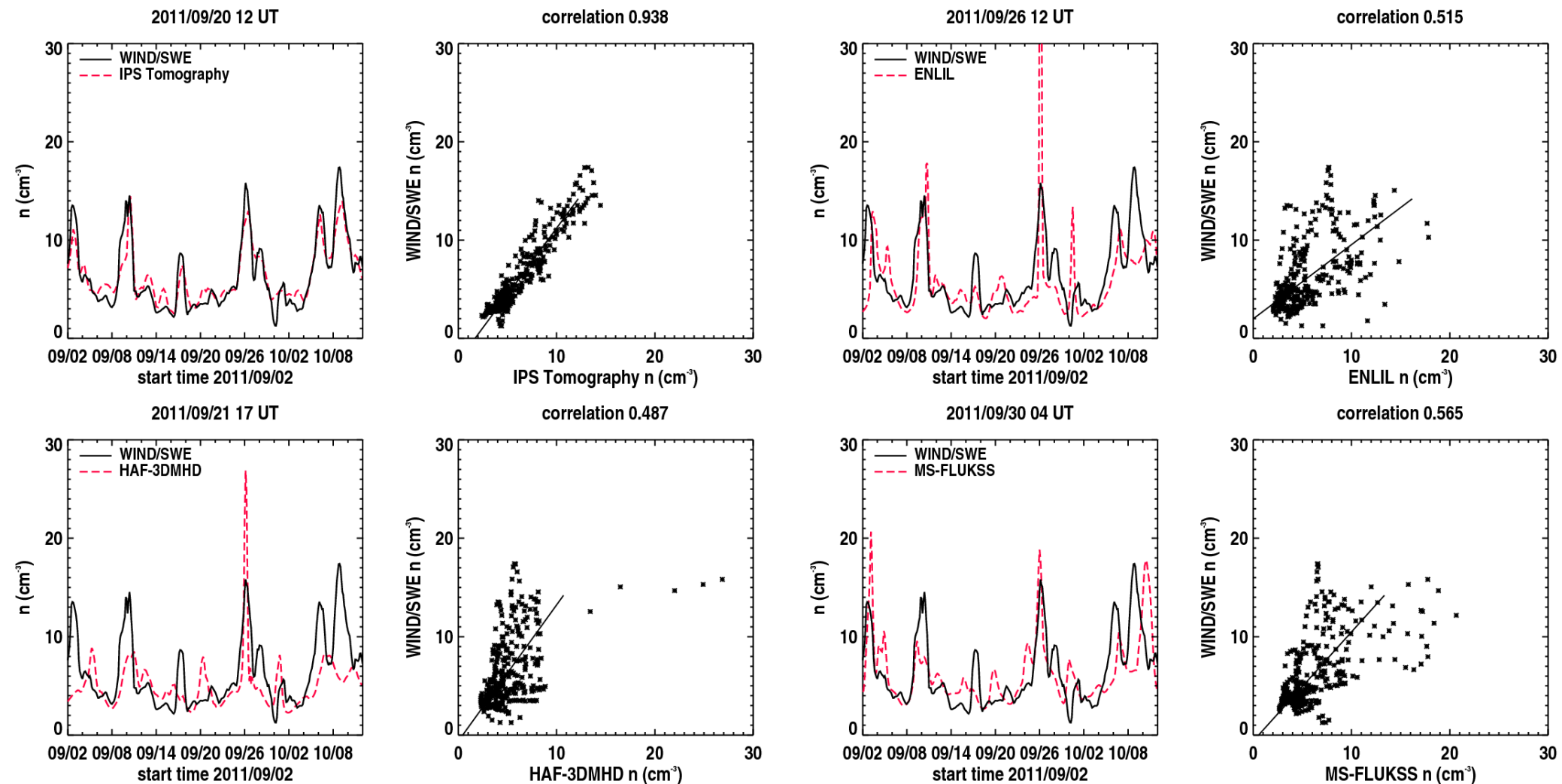
- See, *e.g.* H.-S. Yu, B.V. Jackson, P.P. Hick, A. Buffington, D. Odstreil, C.-C. Wu, J.A. Davies, M.M. Bisi, and M. Tokumaru, “3D Reconstruction of Interplanetary Scintillation (IPS) Remote-Sensing Data: Global Solar Wind Boundaries for Driving 3D-MHD Models”, Solar Physics “Radio Heliophysics: Science and Forecasting” Topical Issue (Guest Editors M.M. Bisi, B.V. Jackson, and J.A. Gonzalez-Esparza), online first, 2015 (and references therein).

UCSD Tomography Velocity Comparisons



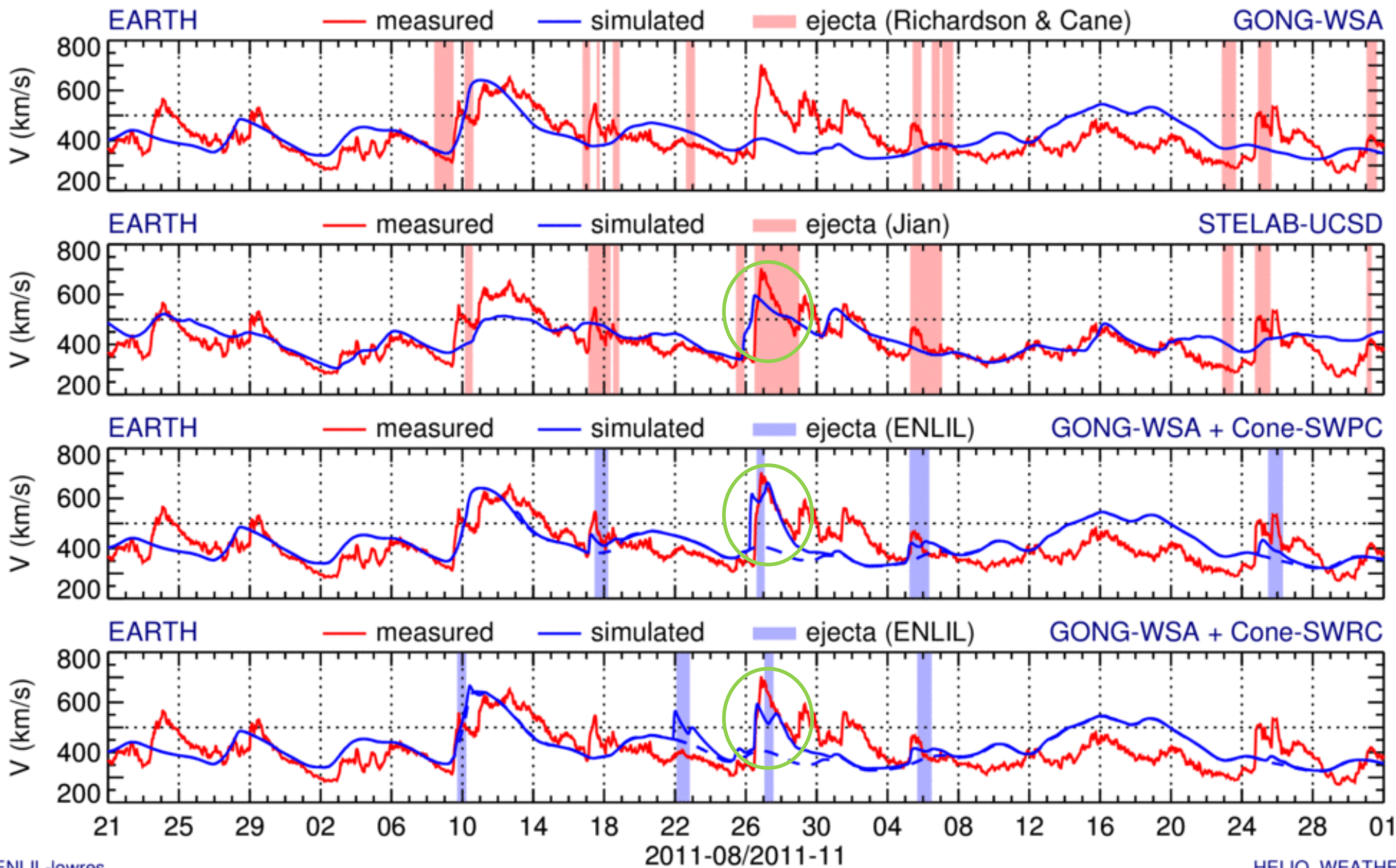
- ❖ Model results by D. Odstrcil (GMU) ENLIL; C.-C. Wu (NRL) HAF-3DMHD; and T. Kim (University of Alabama) MS-FLUXSS.
- ❖ Model Boundaries: UCSD (Kinematic) at 15 R_S , ENLIL (MHD) at 21.5 R_S , HAF-3DMHD at 40 R_S , and MS-FLUXSS (MHD) at $\sim 54 R_S$.

UCSD Tomography Density Comparisons



- ❖ Note, however, that the UCSD kinematic model is both iterative and data-assimilative – these MHD models are not at present.
- ❖ The IPS/*in-situ* kinematic best-fit solution is the one back-projected to the necessary source-surface distance as required in each MHD model.

ENLIL Versions Comparison

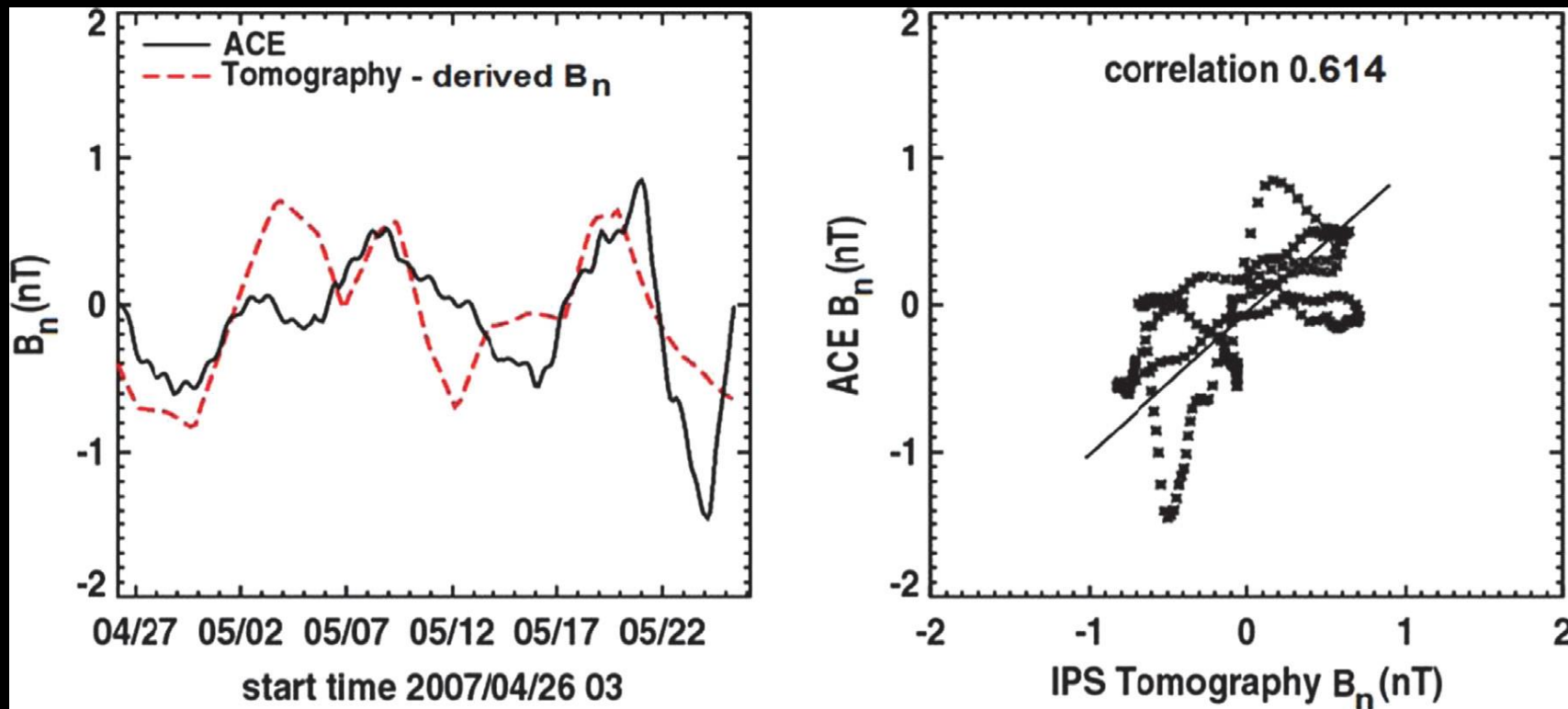


Propagation of Magnetic Fields to 1AU

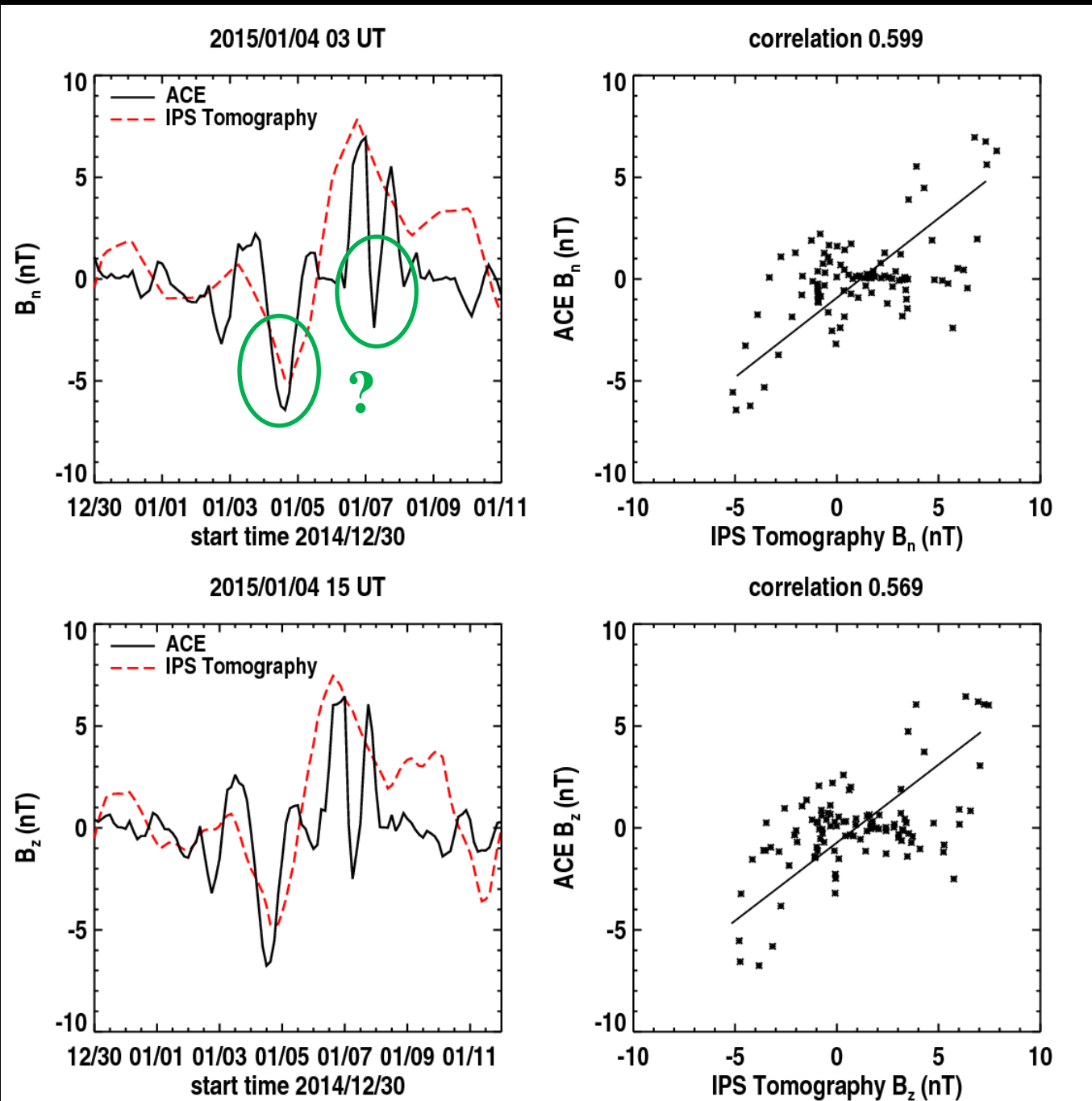
- B.V. Jackson, P.P. Hick, A. Buffington, H.-S. Yu, M.M. Bisi, M. Tokumaru, and X. Xhao, “A Determination of the North-South Heliospheric Magnetic Field Component from Inner Corona Closed-Loop Propagation”, The Astrophysical Journal Letters, 803, L1 (5pp), 2015.
- Other publications in preparation.

And Magnetic-Field Developments (1)

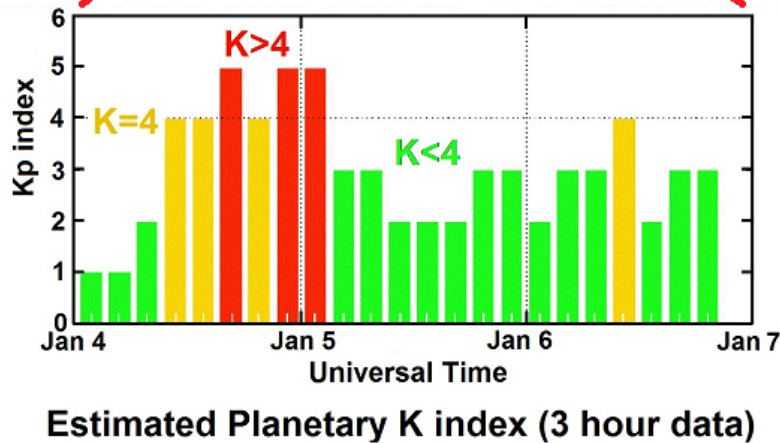
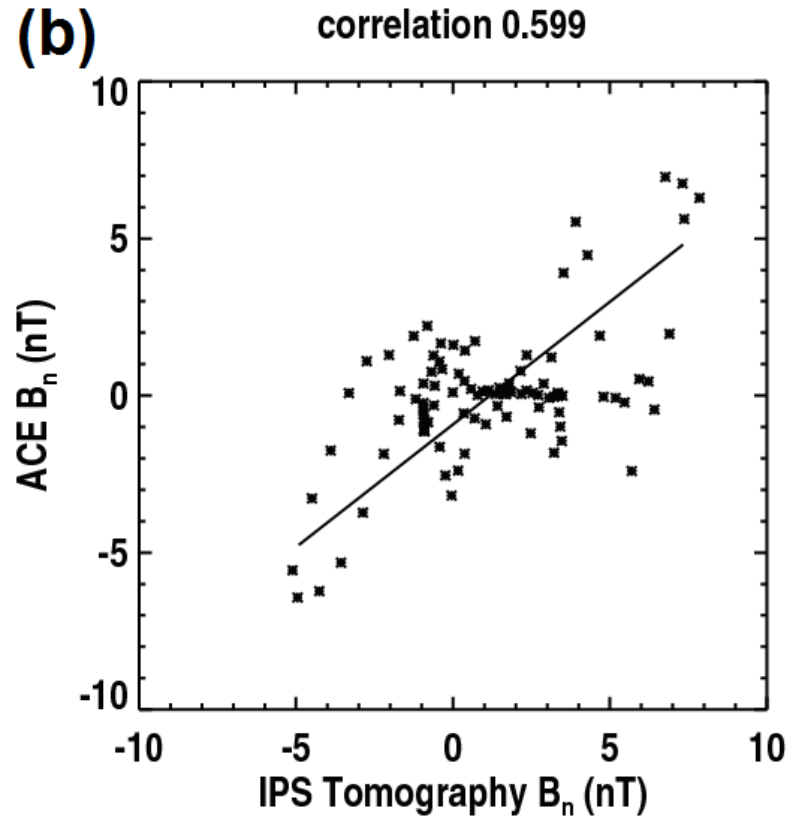
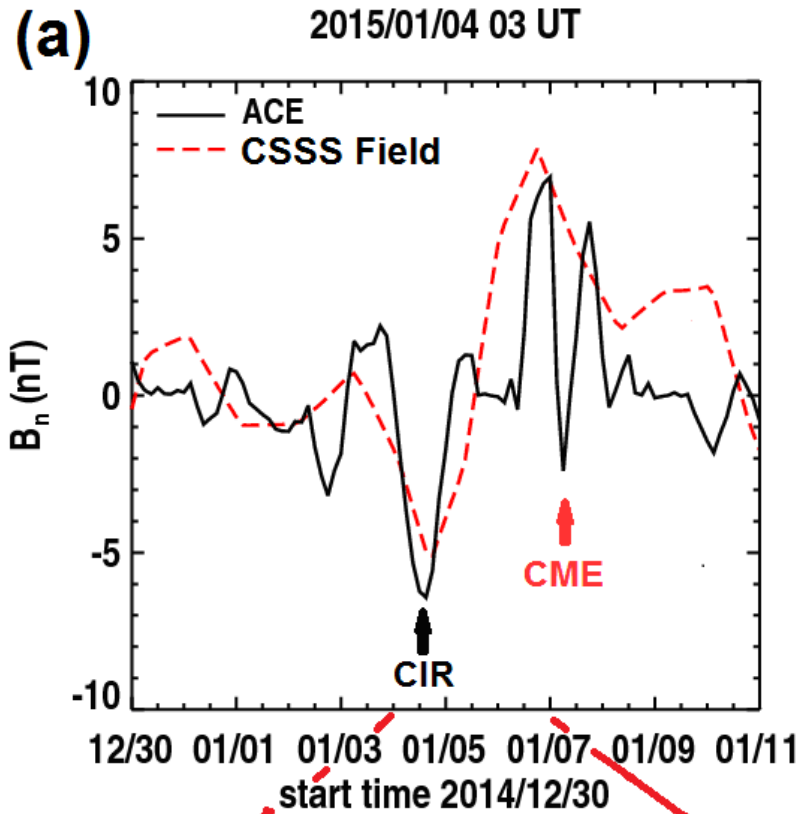
- ❖ With the ability to propagate out ambient magnetic fields from the Sun using the CSSS model, and obtain a reconstruction of B_n (as well as B_t and B_r as previously been obtained) at the Earth, we can compare with *in-situ* data as well as prepare for potential forecasting of RTN magnetic fields near the Earth. This should provide improved inputs for ENLIL and other MHD modelling. In addition, B_z can now be determined at Earth using the UCSD tomography.



And Magnetic-Field Developments (2)

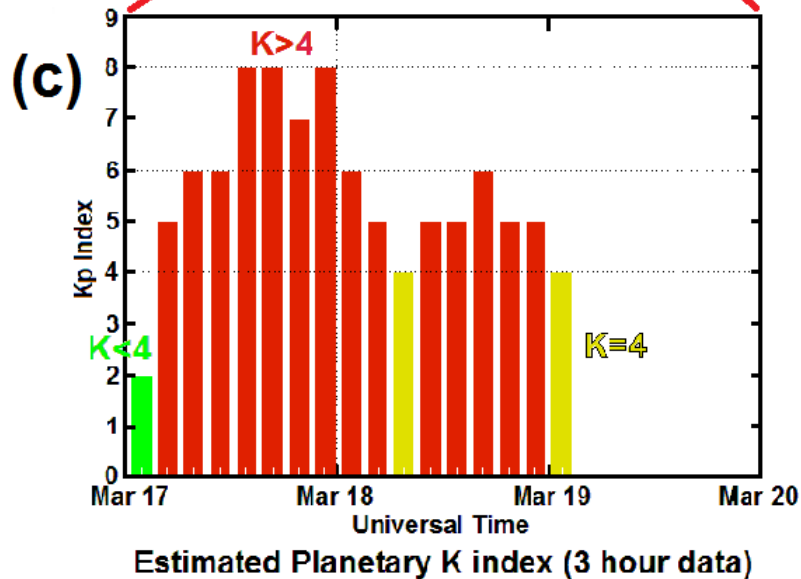
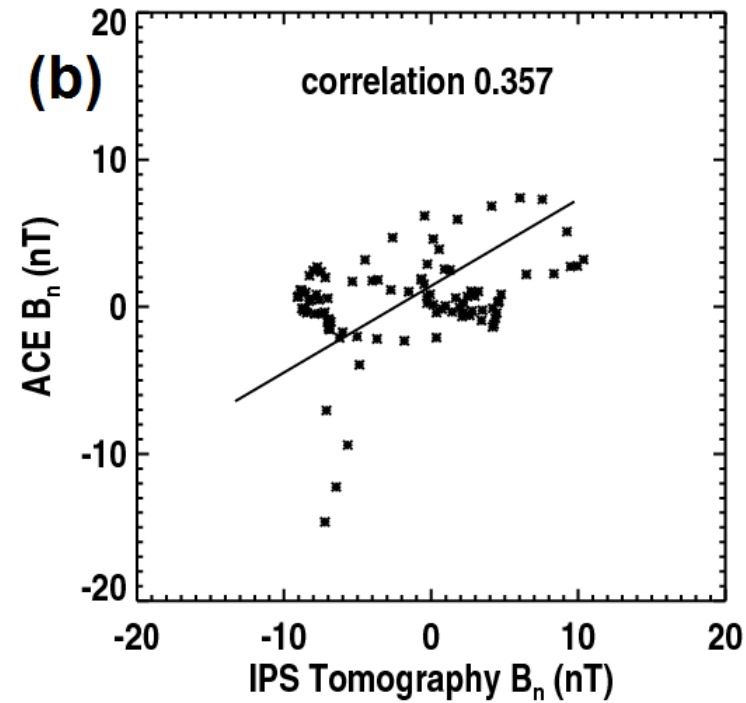
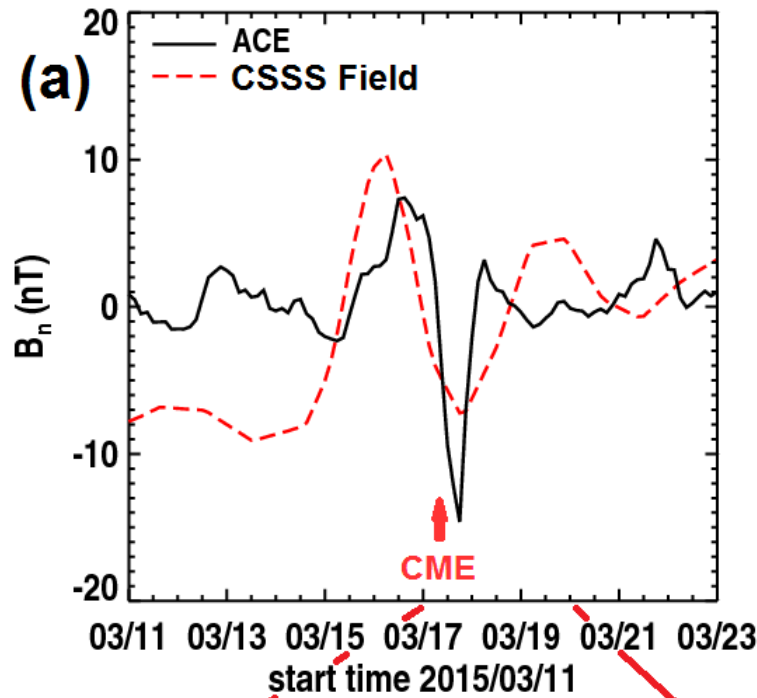


And Magnetic-Field Developments (3)



(c)

And Magnetic-Field Developments (4)



B normal field

Resolution :

Tomo = 0.5 day

ACE = 0.5 day

HELCATS WP7 – T7.1



HELCATS WP7:

**Assessing the complementary nature of
radio measurements of solar wind transients
– Interplanetary Scintillation (IPS) (T7.1)**

Task 7.1 Objectives

- ❖ Started at month 10 (February 2015) for 19.5 months equivalent effort between months 10 and 36.
- ❖ Development of a catalogue of CMEs observed using IPS during the STEREO mission time line and comparison with white-/visible-light observations where geometry allows.
- ❖ As above but for SIRs/CIRs.
- ❖ **Requires HI catalogues with non-changing event IDs.**
- ❖ Primary aspect: EISCAT/ESR and LOFAR individual observations used primarily in conjunction with the HI catalogues.
- ❖ Secondary aspect: where feasible and other IPS data are available (*e.g.* from STELab in Japan), use UCSD tomography and IPS-driven ENLIL on a case-by-case basis for a fuller comparison.
- ❖ Explore how IPS can aid to the investigations of interacting CMEs seen in the STEREO HIs.

Brief Summary

Summary

- ❖ IPS is an extremely powerful and unique technique for making heliospheric imaging observations of the inner heliosphere.
- ❖ Outlook to constraining ENLIL with improved radio heliospheric imaging which might include the background-propagated magnetic-field components: B_x , B_y , and B_z ...
- ❖ IPS/FR on LOFAR is progressing very well with good solar wind/CME results, and preliminary heliospheric RM/FR determination – but much more work to be done and some help needed???
- ❖ The UCSD 3-D tomography should provide an excellent platform for obtaining 3-D magnetic-field values from combined radio observations of FR and IPS and integrating them into the current IPS, closed-loop fields, and L_1 *in-situ* data (and input to ENLIL).